J Am Oil Chem Soc (2007) 84:1053–1062
DOI 10.1007/s11746-007-1132-7

ORIGINAL PAPER

Preparation of Protein-Stabilized β-Carotene Nanodispersions by Emulsification–Evaporation Method

Boon-Seang Chu · Sosaku Ichikawa · Sumiyo Kanafusa · Mitsutoshi Nakajima

Received: 18 April 2006 / Revised: 29 August 2007 / Accepted: 30 August 2007 / Published online: 9 October 2007

Abstract This work was initiated to prepare protein-stabilized β-carotene nanodispersions using emulsification–evaporation. A pre-mix of the aqueous phase composed of a protein and hexane containing β-carotene was subjected to high-pressure homogenization using a microfluidizer. Hexane in the resulting emulsion was evaporated under reduced pressures, causing crystallization and precipitation of β-carotene inside the droplets and formation of β-carotene nanoparticles. Sodium caseinate (SC) was the most effective emulsifier among selected proteins in preparing the nanodispersion, with a monomodal β-carotene particle-size distribution and a 17-nm mean particle size. The results were confirmed by transmission-electron microscopy analysis. SC-stabilized nanodispersion also had considerably high ζ-potential (–27 mV at pH 7), suggesting that the nanodispersion was stable against particle aggregation. Increasing the SC concentration decreased the mean particle size and improved the polydispersity of the nanodispersions. Nanodispersions prepared with higher β-carotene concentrations and higher organic-phase ratios resulted in larger β-carotene particles. Although increased microfluidization pressure did not decrease particle size, it did improve the polydispersity of the nanodispersions. Repeating the microfluidization process at 140 MPa caused the nanodispersions to become polydisperse, indicating the loss of emulsifying capacity of SC due to protein denaturation.

Keywords β-Carotene · Emulsification–evaporation · Nanodispersion · Sodium caseinate

B.-S. Chu · M. Nakajima
National Food Research Institute, Kannondai 2-1-12, Tsukuba, Ibaraki 305-8642, Japan

S. Ichikawa · S. Kanafusa · M. Nakajima (✉)
Graduate School of Life and Environmental Sciences, University of Tsukuba, Tennodai 1-1-1, Tsukuba, Ibaraki 305-8572, Japan
e-mail: mnaka@sakura.cc.tsukuba.ac.jp

Introduction

Nutraceuticals are bioactive compounds, which provide medicinal or health benefits, including the prevention and treatment of diseases [1]. Numerous bioactive compounds with special functionalities have been identified, and their specific beneficial physiological effects are being studied [2–4]. High purity nutraceutical products are available in the marketplace in the forms of capsules and tablets, or being fortified in various food products. However, it has become increasingly evident that these developments alone may not allow us to fully enjoy the nutritional benefits from many of these bioactive compounds because of their low bioavailability [5, 6]. This is particularly true for the water-insoluble lipophilic bioactive compounds [6].

For absorption to be possible in the gastro-intestinal tract, achieving a solution of the compound of interest in the gastro-intestinal fluid is a critical requirement for a poorly water-soluble compound. Many lipophilic bioactive compounds have aqueous solubility <0.1 mg/ml and often present dissolution limitations to absorption [7]. The Noyes–Whitney dissolution model shows that, the surface area, among others, plays an important role in determining in vivo dissolution rate [7]. The dissolution rate is directly proportional to the surface area of the compound, which in turn increases with decreasing particle size. Moreover, for a smaller particle, the diffusion distance is reduced, resulting in a higher concentration gradient [8]. A high

concentration gradient between the surface of the particle and the bulk solution—according to Fick's law—increases mass flux away from the particle surface [8].

Micronization/milling to micron or submicron particle size ranges is one approach for enhancing the dissolution rates of lipophilic bioactive compounds [9]; however, milling is unsuitable for producing monodispersed systems with narrow particle size distributions [10]. Furthermore, with decreasing particle size, it becomes more difficult to apply mechanical energy in the form of shearing and cavitation forces without simultaneously inducing particle agglomeration [10]. Other problems include contamination of grinding materials [11], very time-consuming, and formation of amorphous domains in crystalline of the compounds due to prolonged milling [12]. Therefore, it is of great interest for developing more effective alternatives to prepare the lipophilic bioactive compound dispersions.

The progress in nanotechnology offers possible solutions for improving the water solubility and bioavailability of the lipophilic bioactive compounds. In the pharmaceutical industry, various methods have been developed to prepare lipophilic bioactive-compound nanodispersions with fine particle diameters in the nano-size range such as emulsification–evaporation, emulsification–diffusion, solvent displacement, and precipitation methods [10]. Although most of the methods are in the development stage, they enable preparing extremely fine particulate nanodispersions, and allow continuous and controllable production [10]. Emulsification–evaporation is one of the most popular methods for preparing nanodispersions. With this method, the active compound is dissolved in a lipophilic solvent, and an oil-in-water (O/W) emulsion is formed by emulsifying the active-compound solution with the aqueous phase containing an emulsifier. Converting the emulsion into nanodispersion is then carried out by evaporating the solvent. Precipitation or crystallization of the active compound takes place in the O/W emulsion droplets during evaporation when the solubility limit is crossed. Removal of the solvent from the emulsion droplets decreases the particle size to the nano-size range. The particle morphology is usually polycrystalline in the thermodynamically stable crystal structure, since the solid formation takes place by evaporation crystallization at low supersaturation [10, 13].

The bioactive-compound particles in nanodispersions are stabilized by an emulsifier or a combination of emulsifiers. The emulsifier molecules adsorb at the interface between the two phases, lowering the interfacial tension and preventing or slowing the aggregation of particles of the dispersed phase by increasing repulsion forces between the particles. In spite of successful elaboration of the emulsifiers in stabilizing dispersions, many are restricted to food applications [6]. Food proteins are widely used in formulated foods because they have high nutritional value and are generally recognized as safe [6]. Food proteins, such as caseins, whey proteins, and soy proteins, are among the most important emulsifiers used to prepare food emulsions. Proteins are large complex amphipathic molecules containing combinations of ionic, polar, and non-polar regions; thus, they are surface-active and strongly interact with other food compounds [14]. The interfacial membranes formed by proteins are electrically charged; hence, the major mechanism preventing particle aggregation in protein-stabilized dispersions is electrostatic repulsion [15].

β-Carotene was used in the present work as a model of lipophilic bioactive compounds because it is a common food ingredient and plays important roles in protection against free radical-mediated degenerative diseases such as cancer, macular degeneration, and heart disease [16]. Our previous works have demonstrated that β-carotene nanodispersion can be successfully produced by an emulsification–evaporation technique using Tween 20 or polyglycerol esters of fatty acids as the emulsifier [17, 18]. In the present work, β-carotene nanodispersions were prepared with selected food proteins using the same technique. The primary objectives were to investigate the performance of the proteins in stabilizing the nanodispersion and to determine the effects of operating parameters on the properties of the β-carotene nanodispersion.

Materials and Methods

Materials

Sodium caseinate (SC), β-carotene, and sodium azide were purchased from Wako Pure Chemical Industries, Ltd, Osaka, Japan. Food-grade whey protein concentrate (WPC, 34% protein purity) and whey protein isolate (WPI, 92–95% protein purity) were contributed by Behn Meyer Foodtech Pte. Ltd, Kuala Lumpur, Malaysia; whey protein hydrolysate A (WPH-A, degree of hydrolysis 8.1%, 91% protein purity) and hydrolysate B (WPH-B, degree of hydrolysis 18.1%, 96% protein purity) by Fonterra (NZ) Ltd, Auckland, New Zealand; and soy protein isolate (SPI, >90% protein purity) by Gulf Chemicals Pte. Ltd, Selangor, Malaysia. Deionized water purified by a Milli-Q Organex system (Millipore, Bedford, CT, USA) was used for preparing the aqueous phase. All other chemicals used were analytical grade.

Preparation of the β-Carotene Nanodispersions

Unless otherwise specified, β-carotene nanodispersions were prepared by the following method. Protein (1 wt%)

was dissolved in 0.05 M phosphate buffer pH 7 (at 20 °C), containing 0.02 wt% sodium azide. The aqueous solution was magnetically stirred for 5 h before the organic phase (0.1 wt% β-carotene in hexane) was added. The ratio of organic phase to aqueous phase was 1:9 by weight. The pre-mix was homogenized using a conventional homogenizer (Polytron® PT300, Kinematica AG, Lucerne, Switzerland) at 5,000 rpm for 5 min to produce a coarse O/W emulsion, immediately followed by microfluidization (Model M-110EH Microfluidizer Processor, Microfluidic™ Corporation, Newton, ME, USA) in a single pass at 140 MPa [17, 18]. Fifty microliter of emulsion was then evaporated using a rotary evaporator (Eyela NE-1101, Tokyo Rikakikai Co., Ltd, Tokyo, Japan) at 45 °C under programmed pressures (reducing the pressure from 1,000 to 500 HPa at –20 HPa min^{-1}, holding for 5 min, reducing the pressure from 500 to 100 HPa at –10 $HPamin^{-1}$, holding for 5 min, reducing the pressure from 100 to 50 HPa at –5 $HPamin^{-1}$ and hold for 15 min). Hexane and some of the water were evaporated, and the nanodispersion was concentrated five times.

SC-stabilized β-carotene nanodispersions were prepared under various operating conditions to determine the effects of the experimental parameters on the particle size of the nanodispersions (Table 1). The SC concentration was varied from 0.05 to 5 wt% to determine the effect of the protein concentration. Nanodispersions of various β-carotene concentrations (0.05 to 0.3 wt% in hexane) were also produced, while several other nanodispersions were prepared under different microfluidization pressures (20 –160 MPa) and microfluidization cycles (1–3 cycles at 140 MPa). The effect of the ratio of organic phase to aqueous phase was determined by varying the ratio of the two phases from 1:9 to 3:7 (by weight). Each nanodispersion was analyzed for particle-size distribution.

Particle-size Analysis

A laser-diffraction particle-size analyzer with the lowest measuring limit of 40 nm (LS 13320, Beckman Coulter, Inc., FL, USA) was used to measure the droplet size distribution of the initial emulsions (before hexane evaporation). After evaporating the hexane, the particle size decreased to the nano-size range. Mean particle diameter and particle-size distribution of the nanodispersions were measured using a dynamic light-scattering particle-size analyzer that had a measuring range of 0.6 nm–6 μm (Zetasizer Nano ZS, Malvern Instruments Ltd, Worcestershire, UK). For both instruments, a refractive index of 1.47 for β-carotene in polar solution (water) [19] and that of 1.33 for water were used to calculate the droplet or particle size. For the dynamic light-scattering particle-size analyzer, the sample was diluted with phosphate buffer (pH 7) prior to analysis, so that the final particle concentration was 0.005 wt%, to avoid multiple scattering effects during the measurement [20]. The absorbance of the nanodispersion particle was set at 0.3 (colored particle at 633 nm), and the temperature was 25 °C. The final particle diameter was calculated from the mean of at least three measurements. The coefficient of variation (CV) for particle-size distribution was calculated from the standard deviation and mean particle size.

Zeta-potential Measurement

Electrophoretic-mobility measurements were conducted using the Zetasizer Nano ZS (Malvern Instruments Ltd, Worcestershire, UK). The instrument measured distribution of electrophoretic mobility and ζ-potential of nanodispersion particles with a size range of 3 nm–10 μm using the Laser-Doppler Velocity technique. The ζ-potentials of the samples were determined from the electrophoretic mobility by applying the Henry equation. The temperature during measurement was 25 °C. The pH values of the nanodispersions during the measurement of ζ-potential was pH 7. All measurements were taken in duplicate.

Interfacial-tension Measurement

Protein solutions (1 wt%) were prepared by separately dispersing the powdered proteins into 0.05 M phosphate buffer solution at pH 7 and stirring for 5 h at room temperature. Interfacial tension between the protein solution and hexane was determined at room temperature by the pendant-drop method using a tensiometer (FACE Full Automatic Interfacial Tensiometer, model PD-W, Kyowa Interface Science Co., Ltd, Tokyo, Japan). The protein solution was injected with a needle dipped in hexane, so that it formed a drop on the tip of the needle. The drop was then optically observed, and computer software was used to calculate the surface tension from the shape of the drop [21].

Transmission-electron microscopy (TEM) Analysis

The nanodispersions were also observed by TEM for microstructure and particle-size distribution of the β-carotene particles in the nanodispersions. The sample was prepared using the freeze-fracture replica method [22]. The surface of the fractured sample was coated with a platinum layer followed by a carbon layer in vacuum. The metal atoms were applied at 45° to the fractured surface to

Table 1 Experimental design of the parameters

Experiment	Parameter				
	SC concentration (%wt)	β-carotene concentration (%wt)	OP:AP ratio	Microfluidization pressure (MPa)	Microfluidization cycle
Effect of SC concentration	0.05	0.1	1:9	140	1
	0.1	0.1	1:9	140	1
	0.5	0.1	1:9	140	1
	1.0	0.1	1:9	140	1
	5.0	0.1	1:9	140	1
Effect of β-carotene concentration	1.0	0.05	1:9	140	1
	1.0	0.1	1:9	140	1
	1.0	0.2	1:9	140	1
	1.0	0.3	1:9	140	1
Effect of OP:AP ratio	1.0	0.1	1:9	140	1
	1.0	0.1	2:8	140	1
	1.0	0.1	3:7	140	1
Effect of microfluidization pressure	1.0	0.1	1:9	20	1
	1.0	0.1	1:9	60	1
	1.0	0.1	1:9	100	1
	1.0	0.1	1:9	140	1
	1.0	0.1	1:9	160	1
Effect of microfluidization cycle	1.0	0.1	1:9	140	1
	1.0	0.1	1:9	140	2
	1.0	0.1	1:9	140	3

SC Sodium caseinate, *OP*:*AP* organic phase:aqueous phase

produce a shadow effect. TEM images were then obtained using a JEOL-JEM 200CX TEM (JEOL, Tokyo, Japan) working at an accelerating voltage of 80 kV.

Statistical Analysis

Statistical analysis was performed on the data by a one-way analysis of variance using SAS [23] software package release 6.1. The significant differences ($P < 0.05$) between means were further determined by Duncan's multiple-range test. All of the reported values were the means of at least four measurements from two experiment replications.

Results and Discussion

Changes in Particle Size During Emulsification and Evaporation

The β-carotene nanodispersions were prepared by emulsification–evaporation. The β-carotene was first dissolved in hexane before being added to the continuous phase, which was the 0.05 M phosphate buffer containing a protein as the emulsifier. Figure 1 presents an example of the typical changes in the particle diameter after coarse homogenization, microfluidization, and evaporation of SC-stabilized nanodispersion. Coarse homogenization by using a conventional rotor–stator homogenizer resulted in large droplets with a wide droplet size distribution. There were four droplet populations with mean diameters of 87.9, 41.4 3.5 and 0.2 μm, with percentage volumes of 7.1, 79.2, 8.6 and 5.1%, respectively. The primary homogenization involved the breakup and intermingling of bulk β-carotene solution and aqueous phase so that fairly large droplets were formed and dispersed in the aqueous phase. Subsequent microfluidization limited the mean particle diameter in the range of 1.0–20.0 μm with a mean value of 5.7 μm (CV 52.2%), owing to the fact that microfluidization applied higher disruptive energy than the conventional rotor–stator homogenizer. The breakup of the large droplets to smaller ones in the microfluidizer was initiated by a combination of turbulence and laminar-shear stress, which increased the droplet-specific surface area up to disruption. The protein rapidly adsorbed at the surface of the newly formed smaller droplets. The hexane in the droplets was then removed under reduced pressures. Foaming occurred during the evaporation process; a large surface area was crucial for the hexane to evaporate efficiently from the droplets, causing crystallization or precipitation of

β-carotene inside the droplets. As a result, β-carotene particles with a mean diameter of 17 nm were formed.

Effect of Protein Type

Two important functions of emulsifiers during the formation of emulsions/dispersions are: (1) to decrease the interfacial tension between the immiscible phases, thereby reducing the amount of free energy required to disrupt the droplets during emulsification, and (2) to rapidly form a protective coating around the droplets or particles that prevents them from coalescing with each other [15]. Table 2 lists the comparison of the performances of the selected proteins in stabilizing the β-carotene nanodispersion. The proteins greatly lowered the interfacial tension between the aqueous phase and hexane (~40 mNm^{-1} at room temperature), demonstrating their potential for emulsifying the β-carotene solution with water. SC was the most effective emulsifier for preparing the nanodispersion, as indicated by its good capacity in reducing interfacial tension and forming the finest β-carotene particles, with a monomodal particle-size distribution and a low CV of 36%. During emulsification, proteins underwent conformational changes to maximize favorable interactions with the newly formed droplet surfaces. Molecular flexibility and structural packing of the protein determine the time taken for these conformational changes [24, 25]. The caseins, with a relatively lower molecular weight of 19–23 kDa [26], have been described as rheomorphic proteins that adopt molecular structures in solution dictated by the local environment [27]. Molecularly more flexible than other globular proteins, they rapidly adsorbed onto the surface of the droplets and stabilized the dispersion. The

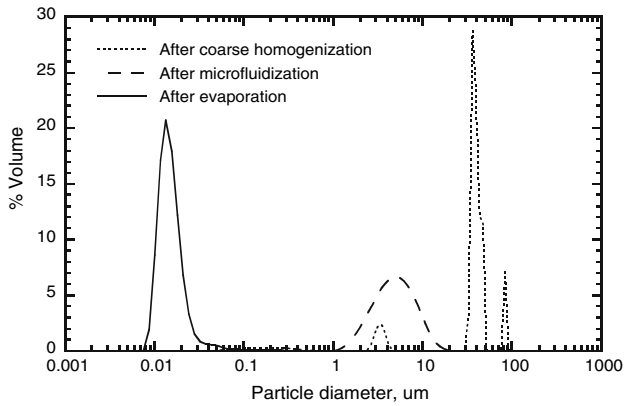

Fig. 1 Typical changes in particle size profile during the preparation of β-carotene nanodispersion. A premix of organic phase and aqueous phase (1:9 by weight) was homogenized using a rotor–stator homogenizer, before it was microfluidizied at 140 MPa for one cycle, and finally the evaporation of hexane

larger and more rigid soy globulins, such as β-conglycinin (7S fraction, ~270 kDa) and glycinin (11S fraction, ~360 kDa) [28] in SPI resulted in nanodispersion with larger β-carotene particles (mean diameter of 196 nm) and wider particle-size distribution (CV 40%), although the profile of particle-size distribution was monomodal. WPC, partly due to its low protein purity (54%), was a relatively poor emulsifier for preparing the nanodispersion, as indicated by its large mean β-carotene particle diameter (145 nm) and high particle-polydispersity nanodispersion (CV 114%). The WPC solution also had significantly ($P < 0.05$) higher interfacial tension with hexane than that of other whey protein counterparts. Higher protein purity implies better emulsifying properties. The WPI (92 to 95% protein purity) solution had a lower interfacial tension with hexane, and WPI-stabilized nanodispersion had a smaller mean-particle size than those of WPC.

Hydrolyzing the protein might further improve the emulsifying performance of whey protein, as suggested by WPH-A and WPH-B. The interfacial tension was significantly decreased ($P < 0.05$) with an increase in degree of protein hydrolysis. The mean particle size decreased from 115 nm (CV 100%) in WPI-stabilized nanodispersion to 30 nm (CV 53%) in that of WPH-B. Limited hydrolysis has been reported to improve emulsifying properties of proteins, due to the increased exposure of hydrophobic areas, protein flexibility, and sufficiently smaller molecular weight to form stable films at the interface [29, 30]. However, it should be noted that extensive hydrolysis of the protein decreased emulsifying ability and emulsion stability [31].

A good emulsifier should prevent the particles in the nanodispersion from aggregation during storage. Measuring the ζ-potential enables predicting the storage stability of the nanodispersions. Generally, the particles of a nanodispersion are less likely to aggregate if the particles of the nanodispersion possess high surface charge. For a physically stable nanodispersion stabilized by an emulsifier solely through electrostatic repulsion, a minimum ζ-potential of ±30 mV is required [32]. The ζ-potential of SC-stabilized nanodispersion was close to –30 mV, suggesting that the β-carotene particles were stable against aggregation during storage. In contrast, WPC-stabilized nanodispersions had lower ζ-potential values. This result could be due to the fact that caseins carry a substantially higher net-negative charge than whey proteins. For example, the two major individual caseins, α_{s1}- and β-caseins, have a net-surface charge of –22 and –15*e* at neutral pH [33], while those of whey protein subunits (e.g. α-lactalbumin and β-lactoglobulin) were –3 and –10*e* [34]. WPC-stabilized nanodispersion had the lowest ζ-potential. However, when the purity of the protein increased, the stability of the nanodispersion was expected to increase

Table 2 Comparison of selected proteins in stabilizing β-carotene nanodispersion[1]

Protein	Interfacial tension[2], mNm^{-1}	Characteristics of β-carotene nanodispersion			
		Mean particle diameter, nm	Particle size distribution profile	% CV	ζ-potential[3], mV
SC	17.2 ± 0.9[d]	17.1 ± 0.9[d]	Monomodal	35.6	–27.0
SPI	23.3 ± 1.7[a]	196.3 ± 24.3[a]	Monomodal	40.0	–22.9
WPC	24.1 ± 1.3[a]	145.3 ± 1.5[b]	Polymodal	113.6	–10.9
WPI	21.2 ± 0.9[b]	115.3 ± 3.4[c]	Polymodal	100.1	–16.8
WPH-A	19.5 ± 1.3[c]	110.3 ± 8.5[c]	Polymodal	99.0	–21.0
WPH-B	17.9 ± 1.1[d]	30.4 ± 2.1[d]	Bimodal	53.1	–24.5

SC Sodium caseinate, *SPI* soy protein isolate; *WPC* whey protein concentrate, *WPI* whey protein isolate, *WPH* whey protein hydrolysate, *CV* coefficient of variation. The degree of hydrolysis of WPH-A and WPH-B were 8.1 and 18.1%, respectively

[1] Nanodispersions were prepared with 1.0 wt% protein and 0.1 wt% β-carotene

[2] Water and hexane interfacial tension was measured at room temperature with the presence of 1.0 wt% protein in the aqueous phase

[3] Zeta-potential was measured at pH 7

Mean values within a column with different superscript letters are significantly ($P < 0.05$) different

accordingly, as indicated by the increase in ζ-potential of WPI-stabilized nanodispersion. Nanodispersions prepared with whey protein hydrolysates (WPH-A and WPH-B) further increased the ζ-potential of the particles, due to the exposure of more electrostatically charged protein sites.

SC was the most suitable emulsifier among the selected proteins for preparing β-carotene nanodispersion. The caseins were distinguished from other food proteins by their excellent emulsifying properties: the ability to significantly lower the interfacial tension between the two phases for ease of emulsification, low molecular weight and structure flexibility for rapid adsorption onto the surfaces of droplets or particles, and considerably large ζ-potential values of the particles formed. The electrostatic and steric stabilizing-casein layer protects fine particles against coalescence and ensures long-term stability during subsequent processing and storage. Therefore, SC was used as the emulsifier when studying the effects of other experiment parameters on the preparation of β-carotene nanodispersion.

Effects of the Nanodispersion Ingredients

Figure 2 shows the effects of initial SC concentration in the aqueous phase on the β-carotene particle size after evaporation of hexane. At low SC concentration (<0.5 wt%), the nanodispersions had large mean particle diameters and wide particle-size distributions. This result was partly due to insufficient SC to completely cover the surfaces of the newly formed droplets during microfluidization. The droplets aggregated with neighboring droplets or particles forming much larger droplets. Increasing the protein concentration in the aqueous phase provided better availability of the emulsifier to stabilize the droplets or particles before they re-aggregated and thereby narrowing the particle size range. The mean particle diameter decreased significantly ($P < 0.05$) from 189 nm (CV 105%) at 0.05 wt% SC to 17 nm (CV 36%) at 1 wt%. However, further increasing the SC concentration to 5 wt% did not significantly change ($P > 0.05$) the mean particle diameter. When the SC concentration was in excess, the particle size was independent of the protein concentration and depended primarily on the energy input of the homogenizer [15]. Nevertheless, excess SC concentration did improve the particle-size distribution, as indicated by a sharper particle-size profile (Fig. 2) and a lower CV of 30% for nanodispersion prepared with 5 wt% SC.

Figure 3 illustrates the effect of initial β-carotene concentration in the organic phase on the particle-size distribution. Microfluidization formed hexane droplets containing dissolved β-carotene. Evaporating the hexane caused the β-carotene to precipitate or crystallize, and the particles formed were bound with the caseinate. The lower the concentration of β-carotene in the hexane, the smaller the β-carotene particle formed after evaporating hexane. These results indicated that increasing the β-carotene concentration significantly increased ($P < 0.05$) the mean particle diameter and its polydispersity. For instance, the mean particle diameter was 15 nm (CV 31%) at 0.05 wt% β-carotene but increased to 45 nm (CV 118%) at 0.3 wt% β-carotene. The particle-size distribution also tended to become bimodal at increased β-carotene concentration, probably due to the failure of SC to bind effectively with the β-carotene particles.

The β-carotene particles exhibited bimodal or polymodal size distributions when the organic or aqueous ratio was increased (Fig. 4). The mean particle diameter also

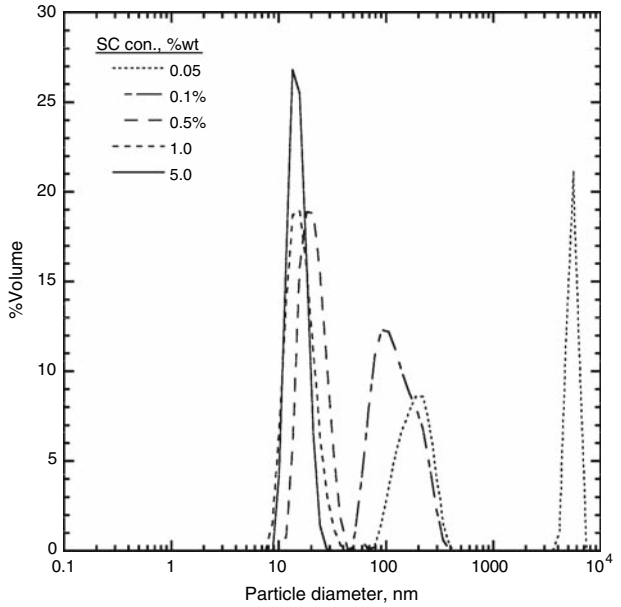

Fig. 2 Effects of sodium caseinate concentration on particle size profile of β-carotene nanodispersions. Ratio of organic:aqueous phases, 1:9 (by weight); initial concentration of β-carotene in the organic phase, 0.1 wt%; microfluidization pressure, 140 MPa for one cycle

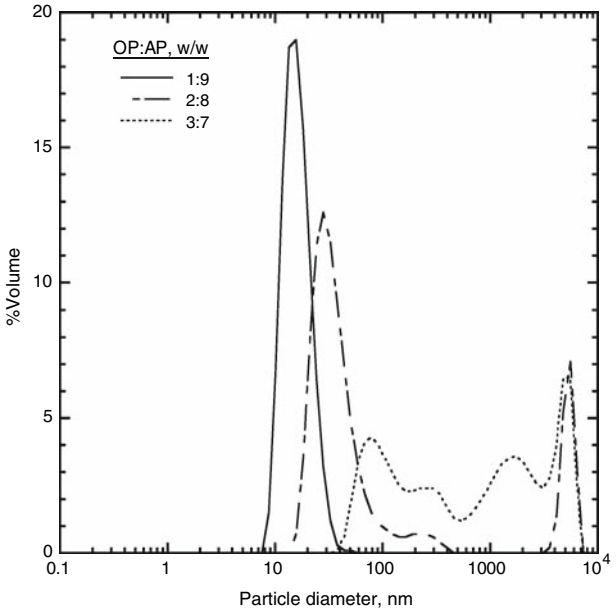

Fig. 4 Effects of organic phase to aqueous phase ratio on the particle profile of β-carotene nanodispersions. Initial concentration of sodium caseinate in the aqueous phase, 1 wt%; initial concentration of β-carotene in the organic phase, 0.1 wt%; microfluidization pressure, 140 MPa for one cycle

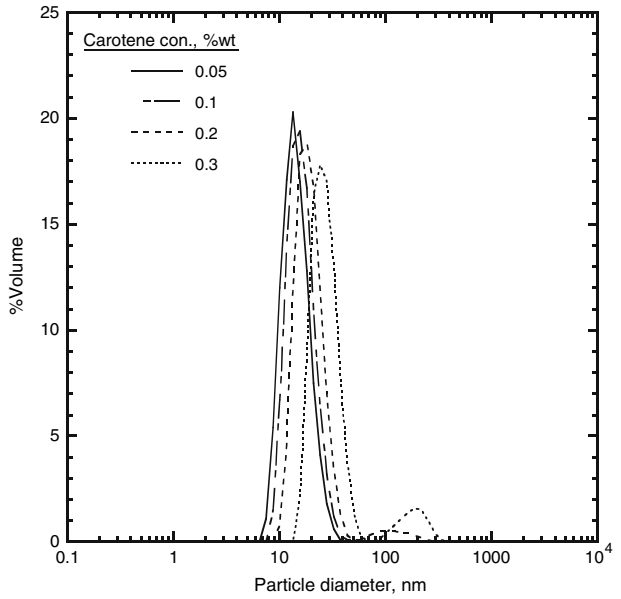

Fig. 3 Effects of β-carotene concentration on particle size profile of β-carotene nanodispersions. Ratio of organic:aqueous phases, 1:9 (by weight); initial concentration of sodium caseinate in the aqueous phase, 1 wt%; microfluidization pressure, 140 MPa for one cycle

increased significantly ($P < 0.05$). Higher organic-phase ratio increased the viscosity of the system, making it less favorable for mixing and reducing shear–stress efficiency during homogenization [17]. At higher viscosity, the droplets resisted breakup because they had insufficient time to become deformed before the disruptive forces caused them to rotate to new orientations [15]. Additionally, at a constant SC concentration in the aqueous phase, the availability of SC per unit organic phase decreased with increasing organic-phase ratio. Newly formed droplets aggregated easily at lower aqueous-phase ratios because the systems lacked SC to stabilize the droplets.

Effect of Microfluidization Parameters

The effect of microfluidization pressure as a function of the β-carotene particle diameter is illustrated in Fig. 5. The particle-size profiles of the nanodispersions had major peaks with mean particle sizes of 16.1 to 17.3 nm, regardless of the microfluidization pressure applied. At high microfluidization pressures (≥100 MPa), the particle-size profiles were monomodal with low particle-size polydispersity values (CV < 40%). Although β-carotene nanodispersions with a particle size of 20 nm could still be prepared at lower pressures (20–100 MPa), the nano-dispersions contained small amounts of particles in submicron and micron sizes. The polydispersity of the nanodispersions increased from CV 40% at 100 MPa to 115% at 20 MPa. Higher microfluidization pressure applied more shear stress and increased the velocity at which the liquid was brought into contact. While increasing the microfluidization pressure from 20 to 160 MPa did not

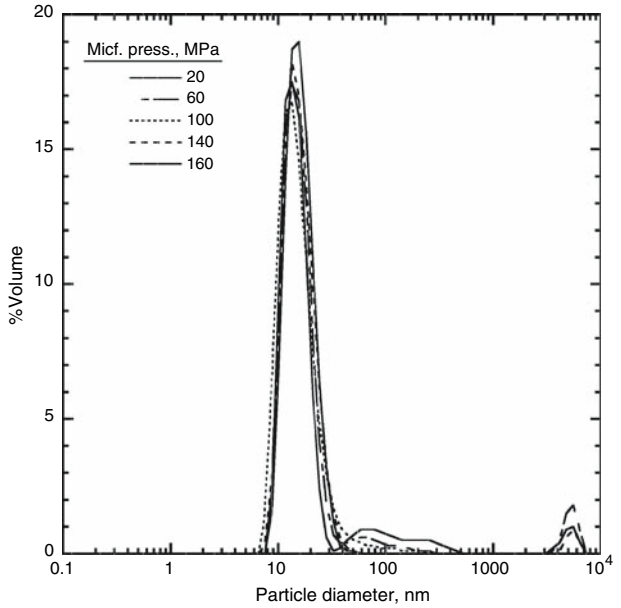

Fig. 5 Effects of microfluidization pressure on the particle size profile of β-carotene nanodispersions. Ratio of organic:aqueous phases, 1:9 (by weight); initial concentration of sodium caseinate in the aqueous phase, 1 wt%; initial concentration of β-carotene in the organic phase, 0.1 wt%

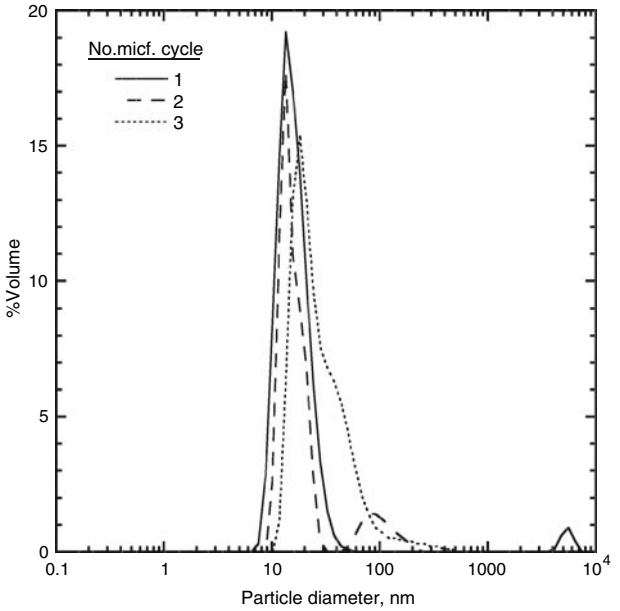

Fig. 6 Effects of microfluidization cycle on the particle size profile of β-carotene nanodispersions. Ratio of organic:aqueous phases, 1:9 (by weight); initial concentration of sodium caseinate in the aqueous phase, 1 wt%; initial concentration of β-carotene in the organic phase, 0.1 wt%; microfluidization pressure, 140 MPa

further decrease the β-carotene particle size in this work, it did improve the polydispersity of the nanodispersions. Furthermore, the effectiveness of SC to stabilize the nanodispersion decreased when it was extensively subjected to high pressure (Fig. 6). The nanodispersions exhibited a bi- or polymodal particle-size distribution when the microfluidization process was repeated at 140 MPa. The mean β-carotene particle size and CV increased from 17 nm and 36% for one microfluidization cycle to 42 nm and 111% for three cycles. Excessive exposure of SC to high pressure denatured the protein, resulting in the loss of its emulsifying properties.

TEM Analysis

A representative TEM image of SC-stabilized nanodispersion prepared with 0.1 wt% β-carotene and 1 wt% SC is presented in Fig. 7. Careful examination of the TEM image indicated that most of the β-carotene particles exhibited spherical morphology with a mean diameter of about 20 nm. These observations closely corresponded with the results observed in the dynamic light-scattering particle-size analysis. These results suggested the β-carotene particles precipitated were stabilized by the casein submicelles (ca. 10 nm in diameter [35, 36]). The particles look like solid objects with a well-defined boundary, in accordance with previous findings that SC submicelles

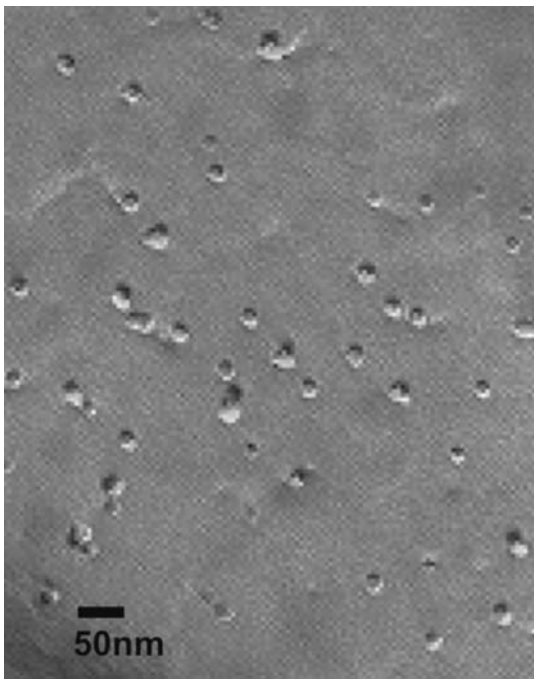

Fig. 7 Transmission electron microscopy image of a typical β-carotene nanodispersion prepared with 1 wt% sodium caseinate. The scale bar represents 50 nm

formed a uniform and smoother adsorption layer at the oil/water interface [37].

SC demonstrated a better potential for preparing the β-carotene nanodispersion than did other selected proteins

using the emulsification–evaporation method. The mean diameters and particle-size distributions of the β-carotene nanodispersions depended on the experimental parameters, especially the SC and β-carotene concentrations and the ratio of organic phase to aqueous phase. Microfluidization parameters also affected the particle-size distribution considerably. Proteins offer a unique challenge for being used as emulsifiers, not only because of the complexity of their molecular structure, but also because of the stability of dispersions during long-term storage and thermal processing. Detailed understanding of the properties of the proteins and their performance as functions of emulsification parameters is important in preparing a stable nanodispersion that meets product requirements.

Acknowledgments The authors gratefully acknowledge the financial support by the Ministry of Agriculture, Forestry and Fisheries of Japan through the Food Nanotechnology Project and the Japan Society for the Promotion of Science for the JSPS Postdoctoral Fellowship awarded to the first author. The authors also thank Ms Fumiko Yukuhiro, Ms Reiko Nagata and Ms Yoko Terai for their kind contributions to this work.

References

1. Clydesdale FM (1997) A proposal for the establishment of scientific criteria for health claims for functional foods. Nutr Rev 55:413–422
2. Carpenter R, O'Grady MN, O'Callaghan YC, O'Brien NM, Kerry JP (2007) Evaluation of the antioxidant potential of grape seed and bearberry extracts in raw and cook pork. Meat Sci 76:604–610
3. Ignarro LJ, Balestrieri ML, Napoli C (2007) Nutrition, physical activity, and cardiovascular disease: an update. Cardiovasc Res 73:326–340
4. Siddhuraju P, Becker K (2007) The antioxidant and free radical scavenging activities of processed Cowpea (*Vigna unguiculata* L. Walp.) seed extracts. Food Chem 101:10–19
5. Spernath A, Aserin A (2006) Microemulsions as carriers for drugs and nutraceuticals. Adv Colloid Interface Sci 128:47–64
6. Chen L, Remondetto GE, Subirade M (2006) Food protein-based materials as nutraceutical delivery systems. Trends Food Sci Technol 17:272–283
7. Hörter D, Dressman JB (1997) Influence of physicochemical properties on dissolution of drugs in the gastrointestinal tract. Adv Drug Deliv Rev 25:3–14
8. Kipp JE (2004) The role of solid nanoparticle technology in the parenteral delivery of poorly water-soluble drug. Int J Pharm 284:109–122
9. Müller RH, Peters K, Becker R, Kruss B (1995) Nanosuspensions for the administration of poorly soluble drugs: stability during sterilization and long-term storage. Proc Int Symp Control Rel Bioact Mater 22:574–575
10. Horn D, Rieger J (2001) Organic nanoparticles in the aqueous phase-theory, experiment and use. Angew Chem Int Ed 40:4330–4361
11. Krause KP, Kayser O, Mader K, Gust R, Müller RH (2000) Heavy metal contamination of nanosuspensions produced by high-pressure homogenization. Int J Pharma 192:169–174
12. Willart JF, de Gusseme A, Hemon S, Odou G, Danede F, Descamps M (2001) Direct crystal to glass transformation of trehalose induced by ball milling. Solid State Commun 119:501–505
13. Sjöström B, Bergenståhl B (1992) Preparation of submicron drug particles in lecithin-stabilized O/W emulsions: I. Model studies of the precipitation of cholesteryl acetate. Int J Pharm 84:107–116
14. Dickinson E (1999) Adsorbed protein layers at fluid interfaces: interactions, structure and surface rheology. Colloids Surf B 15:161–176
15. McClements DJ (2005) Emulsion formation. In: food emulsions: principles, practices, and techniques, 2nd edn. CRC Press, pp 95–173, 233–267
16. Che Man YB, Tan CP (2003) Carotenoids In: Gunstone FD (ed) Lipids for functional foods and nutraceuticals, Oily Press, Bridgwater, pp 25–52
17. Tan CP, Nakajima M (2005) β-Carotene nanodispersions: preparation, characterization and stability evaluation. Food Chem 92:661–671
18. Tan CP, Nakajima M (2005) Effect of polyglycerol esters of fatty acids on physicochemical properties and stability of β-carotene nanodispersions prepared by emulsification/evaporation method. J Sci Food Agric 85:121–126
19. Bialek-Bylka GE, Jazurek B, Dedic R, Hala J, Skrzypczak A (2003) Unique spectroscopic properties of synthetic 15-*cis* beta-carotene, an important compound in photosynthesis, and a medicine for photoprotective function. Cell Mol Bio Lett 8:689–697
20. Coupland JN, McClements DJ (2001) Droplet size determination in food emulsions: comparison of ultrasonic and light scattering methods. J Food Eng 50:117–120
21. Xu Q, Nakajima M, Nabetani H, Ichikawa S, Liu X (2001) Effect of the dispersion behavior of a nonionic surfactant on surface activity and emulsion stability. J Colloid Interface Sci 242:443–449
22. Yan Y, Zhang N, Qub C, Liu L (2005) Microstructure of colloidal liquid aphrons (CLAs) by freeze-fracture transmission electron microscopy (FF-TEM). Colloids Surf A 264:139–146
23. SAS (1989) Statistical analysis system user's guide: statistics. SAS Institute Inc., Cary, pp 125–154
24. McClements DJ (2004) Protein-stabilized emulsions. Curr Opin Colloid Interface Sci 9:305–313
25. Freer EM, Yim KS, Fuller CG, Radke CJ (2004) Interfacial rheology of globular and flexible proteins at the hexadecane/water interface: comparison of shear and dilatation deformation. J Phys Chem B 108:3835–3844
26. Dalgleish DG (1998) Casein micelles as colloids: surface structures and stabilities. J Dairy Sci 81:3013–3018
27. Dickinson E, Eliot C (2003) Aggregated casein gels: interactions, rheology and microstructure. In: Proceeding of the 3rd international symposium on food rheology and structure. Zurich, Switzerland, pp 37–44
28. Pearson AM (1983) Soy proteins, In: Hundson BJF (ed) Developments in food proteins 2, Applied Science Publishers, Essex, pp 67–108
29. Foegeding EA, Davis JP, Doucet D, McGuffey MK (2002) Advances in modifying and understanding whey protein functionality. Trends Food Sci Technol 13:151–159
30. Christiansen KF, Vegarud G, Langsrud T, Ellekjaer MR, Egelandsdal B (2004) Hydrolyzed whey proteins as emulsifiers and stabilizers in high-pressure processed dressings. Food Hydrocolloids 18:757–767
31. Agboola SO, Dalgleish DG (1996) Enzymatic hydrolysis of milk proteins used for emulsion formation. I: kinetics of protein breakdown and storage stability of the emulsions. J Agric Food Chem 44:3631–3636

32. Müller RH, Jacobs C, Kayser O (2001) Nanosuspensions as particulate drug formulations in therapy: rationale for development and what we can expect for the future. Adv Drug Deliv Rev 47:3–19
33. Dickinson E, Semenova MG, Antipova AS (1998) Salt stability of casein emulsions. Food Hydrocolloids 12:227–235
34. Swaisgood HE (1996) Characteristics of milk. In: Fennema OR (ed) Food chemistry, 3rd edn. Marcel Dekker, New York, pp 841–878
35. McMahon DJ, McManus WR (1998) Rethinking casein micelle structure using electron microscopy. J Dairy Sci 81:2985–2993
36. Farrell HM Jr, Kumosinki TF, King G (1994) Three-dimensional molecular modeling of bovine caseins: energy-minimized submicelle structure compared with small-angle X-ray scattering data. In: Kumosinki TF, Liebman MN (eds) Am. Chem. Soc. Symp. Ser. 576, American Chemical Society, Washington DC, pp 392–419
37. Krog N., Barfod NM, Sanchez RM (1989) Interfacial phenomena in food emulsions. J Disper Sci Technol 10:483–504